

DETECTION OF NON-DYNAMIC BLEBBING SINGLE UNATTACHED HUMAN EMBRYONIC STEM CELLS

Benjamin X. Guan, Bir Bhanu, Prudence Talbot, Sabrina Lin**

Center for Research in Intelligent Systems, *Stem Cell Center

University of California, Riverside, CA 92521/USA

Email: {xguan001, bhanu}@ee.ucr.edu, {prudence.talbot, sabrina.lin}@ucr.edu

ABSTRACT

Human Embryonic Stem Cells (HESCs) are promising for the treatment of many diseases and for toxicological testing. There is a great interest among biologists to automatically determine the number of various types of cells in a population of mixed morphologies. This study addresses quantification of non-dynamic blebbing single unattached human embryonic stem cells (NDBSU-HESCs) that are in suspension and do not show evidence of blebbing. Current image processing methods are inadequate for detecting these cells in real time. In this paper, we propose a method for NDBSU-HESC detection by using multiple trained classifiers where each classifier eliminates cells with properties unmatched to NDBSU-HESCs. The paper validates the method with many videos captured with live stem cells.

Index Terms— Video Bioinformatics, Phase contrast images

1. INTRODUCTION

Video Bioinformatics is an emerging field to provide a solution to biologists' need for faster and easier ways to analyze large volumes of video data. The biologists who study human embryonic stem cells (HESCs) have to deal with stem cell videos every day, and the analysis of videos is a laborious manual process. It is important to use the information from time lapse videos to study HESCs' behavior during exposure to various chemical agents.

Most stem cell videos are taken with the phase contrast microscopy. It is challenging to analyze these videos automatically. The low signal to noise ratio (SNR) of the phase contrast images makes it hard to analyze the contents in the image and detect non-dynamic blebbing single unattached human embryonic stem cells (NDBSU-HESCs) [5]. Figure 1 shows non-dynamic blebbing, dynamic blebbing, apoptotic dynamic blebbing and dead cell in videos. The NDBSU-HESC is the earliest stage of a cell before attaching to any chemical agents [3]. Hence, it is important to detect these cells accurately before/after treating them with chemicals.

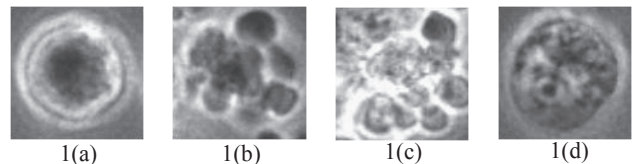


Figure 1(a) Non-dynamic blebbing unattached cell; 1(b) Dynamic blebbing; 1(c) Apoptotic dynamic blebbing; 1(d) Dead Cell.

The proposed method in this paper has three steps for the detection of NDBSU-HESCs; inner cell region detection, feature-based classification and NDBSU-HESC identification. The first step finds inner regions of the NDBSU-HESCs. The second step determines the credibility of the found inner regions based on their size, eccentricity and convexity [2]. The third step identifies NDBSU-HESCs by performing a correlation analysis between the target region and the training data.

2. RELATED WORK AND CONTRIBUTIONS

Existing papers detect cells in phase contrast images under simple environment [4] [7]. Eom et al. [4] discuss two methods for cell detection: detection by circular Hough transform (CHT) and detection by correlation. The CHT is sensitive to the variations of shape and appearance. Therefore, this method is not viable for the detection of NDBSU-HESC under an environment where dynamic blebbing is occurring. The correlation method [7] is also not suitable for our purpose since it does not work with overlapping cells [4]. Further, we need to detect the NDBSU-HESCs mainly from the cell clusters. The contribution of this paper is a detection method for NDBSU-HESCs in a complex environment where dynamic blebbing of stem cells occur everywhere in a frame.

3. TECHNICAL APPROACH

3.1. Motivation and Problem Formulation

In order to study the effect of toxins on NDBSU-HESCs, we need to detect the presence of these cells in each video frame. The videos are captured with BioStation IM [1]. We are dealing with low SNR phase contrast images of

stem cells that are undergoing dynamic morphological changes (blebbing) and cells that are not changing morphologically. This dynamic blebbing makes the detection of NDBSU-HESCs harder if it happens in a cell cluster. Therefore, the two major problems for detecting NDBSU-HESCs are:

1. Low SNR of phase contrast images.
2. Poor NDBSU-HESC recognition in a mixed population of cells.

To analyze the information in the phase contrast images, we need to know characteristics of the cell regions. We find that cell regions in the phase contrast image have high intensity variation. We use this fact to narrow down the classification regions which are further analyzed and verified. Figure 2 shows the overview of the proposed method.

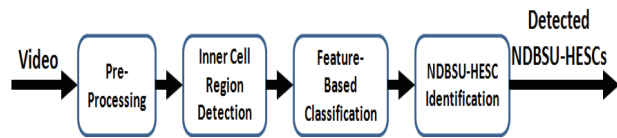


Figure 2: Overview of the Detection Method for NDBSU-HESCs.

3.2. Pre-Processing

A pre-processing procedure is applied to each frame in a video to emphasize intensity differences between the cell regions and the background. I_{oi} is the input image and the pre-processing of I_{oi} is described by the following equations:

$$I_{log} = \log(I_{oi} + 1) \quad (1)$$

The images are normalized by the following equation:

$$I_{log} = \frac{I_{log} - \min(I_{log})}{\max(I_{log}) - \min(I_{log})} \times 255 \quad (2)$$

3.3. Inner Cell Region Detection

Inner cell region detection is a Bayesian classifier that assigns high probability value to the inner regions of the NDBSU-HESCs. Equation (3) shows the principle of our first (Bayesian) classifier [8].

$$P_{(T|W)} = \frac{P_{(T,W)}}{P_{(W)}} = \frac{P_{(W|T)}P_T}{P_{(W)}} \sim P_{(W|T)}P_{(T)} \quad (3)$$

where $P_{(T|W)}$ is a probability of target's intensity, T , given model, w , belongs to the inner cell region. $P_{(W|T)}$ is a given intensity pdfs of NDBSU-HESCs' inner regions, and $P_{(T)}$ is the normalized Euclidean distance, D_n , which is obtained by the following equations discussed below.

Since cell regions have higher intensity variation than the background, we use an entropy based method to separate cell and background regions. The entropy is computed using the gradient magnitude of the image. The gradient magnitude of the image yields more information on high variation regions which are the cell regions, and it is computed using the equation given below:

$$I_{mag} = \sqrt{g_x^2 + g_y^2} \quad (4)$$

where g_x and g_y are gradients of I_{log} in the x and y direction.

After we have obtained I_{mag} , we use it for the entropy calculation and the equation is shown below:

$$I_E(x_1, y_1) = - \sum_{(x,y) \in N_{x_1 y_1}} p_{N_{x_1 y_1}}(x, y) \times \log(p_{N_{x_1 y_1}}(x, y)) \quad (5)$$

where $p_{N_{x_1 y_1}}(x, y)$ is a probability of I_{mag} at the image location $(x, y) \in N_{x_1 y_1}$; $N_{x_1 y_1}$ is a set of neighboring locations of (x_1, y_1) . Equation (5) yields a bimodal image which allows us to find the cell regions easily [2].

The max filter is also used to further enhance the bimodal effects on I_E .

$$I_{max}(x_2, y_2) = \arg \max_{(x,y) \in N_{x_2 y_2}} (I_E(x, y)) \quad (6)$$

I_{max} is the resulting image after max filtering, and $N_{x_2 y_2}$ is a set of neighboring locations of (x_2, y_2) .

With I_{max} found, we obtain a binary image, I_{bi} , by performing a conventional OTSU thresholding on I_{max} , and the result is shown in Figure 3(a) [6]. We know that I_{bi} consists of many individual cell regions. Therefore, we note that R_i is the Euclidean distance transform of the i_{th} region in I_{bi} for $i \in \mathbb{R}$. As the result, we have the following equation as the normalized Euclidean distance transform, D_n , for I_{bi} . D_n is shown in Figure 3(b).

$$D_n = \bigcup_{i \in \mathbb{R}} \frac{R_i}{\max(R_i)} \quad (7)$$

We use D_n as our prior probability to enhance the detection of NDBSU-HESC's inner cell regions. Finally, to reduce the edge effects while emphasize the inner cell regions, equation (3) is modified as equation (8) given below.

$$F(x, y) = \log(P_{(W|T)}(x, y)P_T(x, y) + 1) \quad (8)$$

The final result of Equation (8) is shown in Figure 4(b). Figure 4(a) shows the probability map without the prior probability, D_n .

3.4. Feature-based Classification

Feature-based classification utilizes the normalized probability map, F (equation (8)), found from the previous step to obtain the probable inner cell regions of the NDBSU-HESCs. The classification method uses the area size, eccentricity, and convexity of each probable inner cell region to construct the feature vector. These regions are then passed through a size filter, and regions with undesirable feature values are removed. The filtered regions satisfy one of the following conditions:

- 1) At least one of the region's feature values is greater than the maximum area size, eccentricity, convexity values in the training data.
- 2) A region's size is less than the minimum area size in the training data.

The Euclidean distances of the target's feature vector and the feature vectors in the training data are calculated by:

$$K_f(i) = \begin{cases} \frac{1}{J} \sqrt{\sum_j K_{coef}(i,j)^2} & \sqrt{\sum_j K_{coef}(i,j)^2} \leq J \\ 1 & \text{else} \end{cases} \quad (9)$$

The symbol $K_f(i)$ is the Euclidean distance of the target feature vector and feature vectors from the training data where $i \in \mathbb{R}$. $K_{coef}(i,j)$ is a matrix that contains the differences of the target feature vector and feature vectors in the training data. Since we have three features in our classification method, we have J equal to $\sqrt{3}$ and $j \in \{1,2,3\}$.

The feature-based classification is intended to give us the inner cell regions that have lower Euclidean distance than the defined threshold. This classification step yields centroid locations for the regions for which the minimum of K_f is less than or equal to the user defined threshold.

3.5. NDBSU-HESC Identification

We use contrast stretching and Gaussian filtering on the image to enhance regional similarities. It further segregates the background region from the cell regions. The NDBSU-HESC identification step calculates correlation coefficients for each possible NDBSU-HESC region with all the training data. Each NDBSU-HESC region will have a set of correlation coefficient with the training data. We compare the user defined threshold with the maximum correlation coefficient in that set. We repeat the same process for each possible NDBSU-HESC regions to eliminate unmatched regions. The final result of this classifier is shown in Figure 5.

4. EXPERIMENTAL RESULTS

4.1. Data

We gathered our phase contrast video frames using a BioStation IM. The video frames that we tested our approach on were taken using an objective of 20x with a 600×800 resolution. Each frame is captured every ten minutes.

4.2. Parameters

To estimate the probability map for the NDBSU-HESC regions, we use two parameters for the phase contrast video frames. The first parameter is the acceptable threshold for D_n which is 0.2. The second parameter is the 37×37 processing window for the Bayesian classifier which is the normal size for the inner cell regions. The acceptable minimum Euclidean distance measure for the feature-based classification is 0.51. The maximum acceptable correlation coefficient parameter for the NDBSU-HESC identification step used in this paper is 0.75. All experiments are run with the same four parameters.

4.3. Results

Figure 6 shows the sample frames of video # 1 to 3. Figure 7 compares our estimation of NDBSU-HESCs with the ground truth. Our estimation matches closely with the ground truth. Since video #3 is a toxicity experiment, all healthy cells should be dead eventually. Figure 8 shows the ROC plots for different videos.

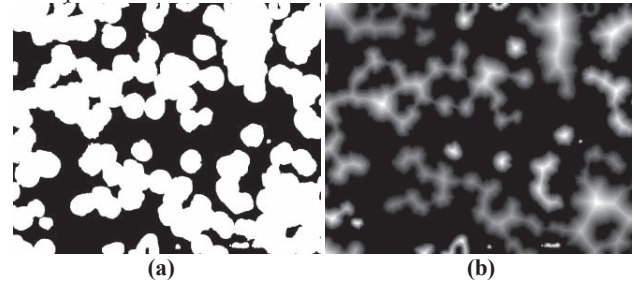


Figure 3: (a) Binary image, (b) Normalized Euclidean dist. of (a)

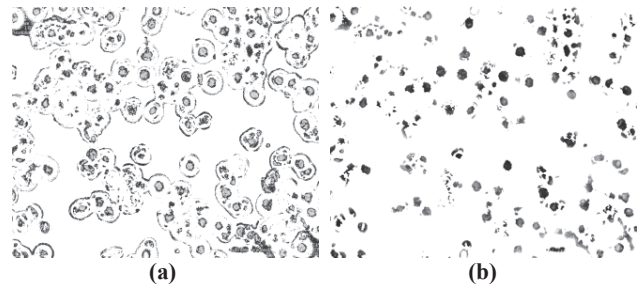


Figure 4: (a) Probability map without the prior probability, (b) Probability map with the prior probability (Color black represents higher probability while color white represents low probability)

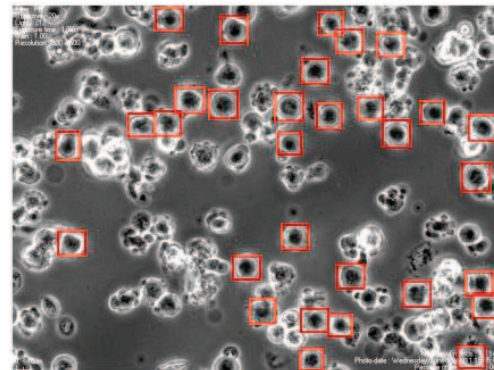


Figure 5: Detected NDBSU-HESCs

5. CONCLUSIONS

NDBSU-HESCs detection by successive elimination of its unmatched properties is plausible. The method yields high true positive rate while it gives low false positive rate. The false positive rate is less than 5% for all the experiments. The method also matches the trend of the ground truth of the experiment closely. To improve the accuracy further, we will investigate into getting more frames per second to establish inter-frame relationships to better estimate the NDBSU-HESC regions.

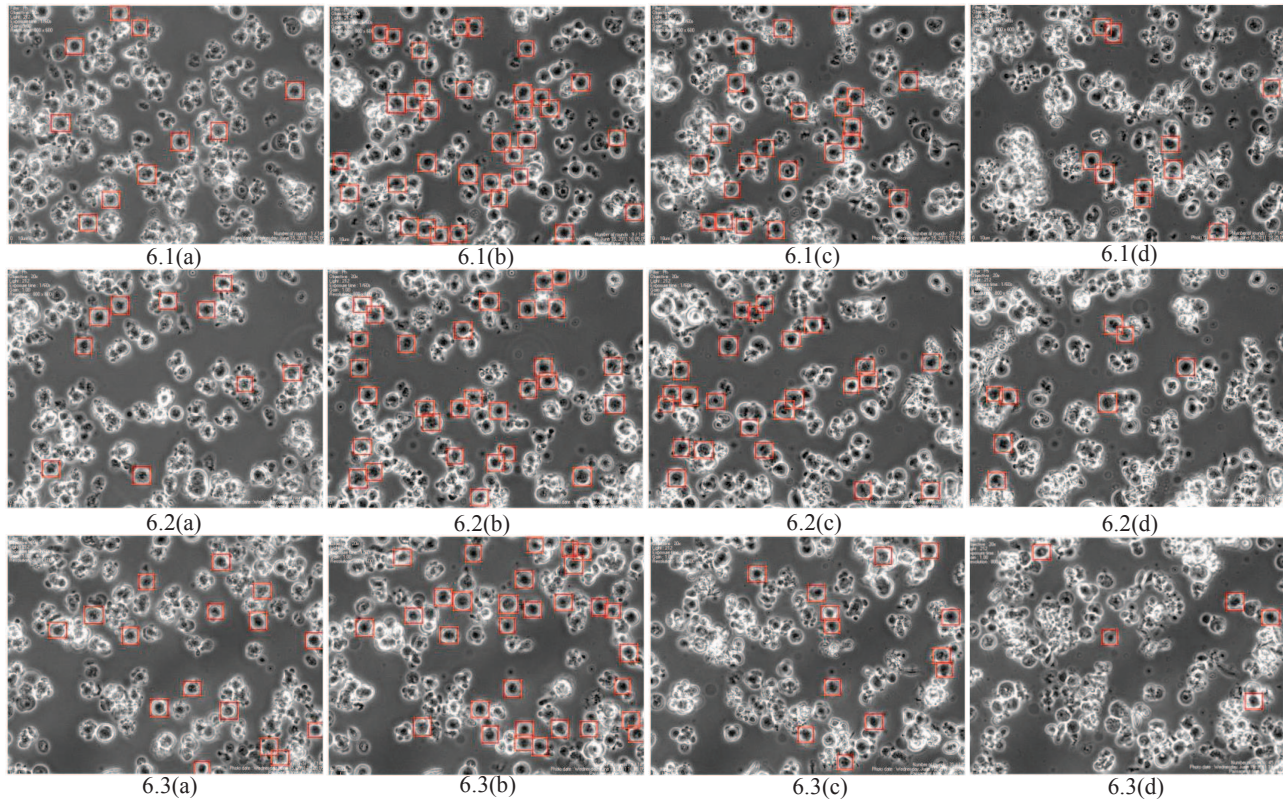


Figure 6: The sample results of video #1, #2 and #3.

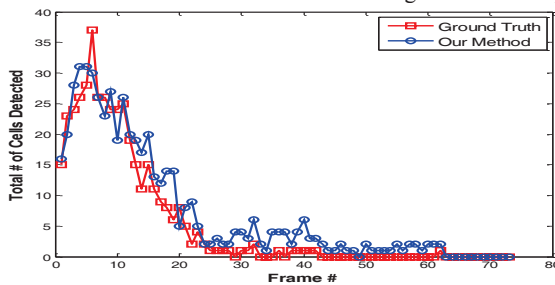


Figure 7: Cell count comparison plots of video #3

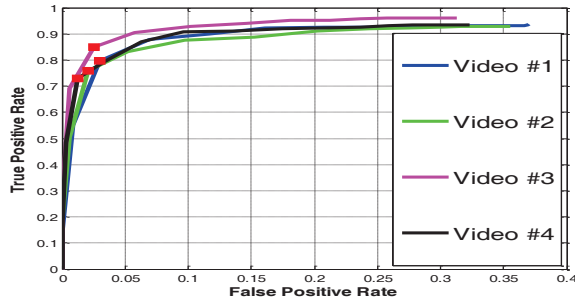


Figure 8: True positive rate vs. false positive rate (ROC Curves: the red squares are the results with our parameters.)

6. ACKNOWLEDGEMENT

This research is supported by NSF IGERT: Video Bioinformatics Grant DGE 0903667 & by TRDRP: Grant 19XT-051.

7. REFERENCES

- [1] BioStation-IM. [Online]. Available: <http://www.nikoninstruments.com/Vyrobky/Cell-Incubator-Observation/BioStation-IM>
- [2] R. C. Gonzalez, R. E. Woods, & S. L. Eddins, *Digital image processing using Matlab*, Prentice Hall, Upper Saddle River, NJ, 2003.
- [3] R. Yu, M. Wu, S. Lin and P. Talbot, "Cigarette smoke toxicants alter growth and survival of cultured mammalian cells," *Toxicological Sciences*, 93(1), pp. 82-95, 2006.
- [4] S. Eom, R. Bise, & T. Kanade, "Detection of hematopoietic stem cells in microscopy images using a bank of ring filters," *Proc. 7th IEEE International Symposium on Biomedical Imaging*, Rotterdam, Netherlands, pp. 137-140, 2010.
- [5] N. Nezamoddini-Kachouie, L. J. Lee, & P.W. Fieguth, "A probabilistic living cell segmentation model," *Proc. 2005 International Conference on Image Processing*, Genoa, Italy, pp. 1137-1140, 2005.
- [6] N. Otsu, "A threshold selection method from gray-level histogram," *IEEE Transaction on Systems, Man and Cybernetics*, 9, pp. 62-66, 1979.
- [7] L. Miroslaw, A. Chorazyczewski, F. Buchholz, & R. Kittler, "Correlation-based method for automatic mitotic cell detection in phase contrast microscopy," *Advances in Intelligent and Soft Computing*, 30, pp. 627-634, 2005.
- [8] Z. Yin, R. Bise, M. Chen, and T. Kanade, "Cell segmentation in microscopy imagery using a bag of local Bayesian classifiers," *Proc. 7th IEEE International Symposium on Biomedical Imaging*, Rotterdam, Netherlands, pp. 125-128, 2010.